Synthesis and Aggregation Behavior of Perylenetetracarboxylic Diimide Trimers with Different Substituents at Bay Positions

Junqian Feng,[†,‡] Baolong Liang,[†] Delou Wang,[†] Haixia Wu,[†] Lin Xue,[†] and Xiyou Li[†,*]

Department of Chemistry, Shandong University, China 250100, and College of Shandong Police, Shandong, China, 250014

Received May 12, 2008. Revised Manuscript Received July 4, 2008

Three perylene tetracarboxylic diimide (PDI) trimers substituted with different side groups at the bay positions were prepared with the triazine ring as a linkage. The free rotation of C−N−C bonds between the triazine ring and the PDI unit provide these molecules with some flexibility. The UV−vis absorption and fluorescence spectra of these three compounds show different concentration-dependent behaviors, which depend on the side groups at the bay positions. Significant aggregation in organic solvents was revealed by the electronic absorption and emission spectra as well as the fluorescence quantum yield calculation. The aggregation behavior of these compounds in the solid state were investigated by X-ray diffraction (XRD), and the morphology of the aggregates was examined by atomic force microscopy (AFM). The aggregation of trimer **1** with two phenoxy groups at the 1 and 7 positions results in long nanofibers whereas trimers **2** and **3** with dipiperidinyl groups or tetraphenoxyl groups at the bay positions form only particles. The results of this research revealed that PDI trimers with flexible structures can also self-assemble into large ordered aggregates such as those with rigid structure. This information is believed to be useful in the design of novel nanoorganic materials.

Introduction

Perylene tetracarboxylate diimides (PDI) are currently being investigated for use in a variety of photoactive organic materials because of their excellent thermal and light stability, high luminescence efficiency, and optoelectronic properties.[1−3] They have generated great interest in organic field-effect transistors, light-harvesting solar cells, and robust organic dyes that are resistant to photobleaching.[4−13] Because of the strong $\pi-\pi$ interactions between the planar PDI rings, they have been proven to be excellent building blocks for self-organized molecular materials with highly ordered structure.[14−34]

Recently, a strategy has been developed in the design of self-organized organic material by connecting several planar conjugated organic molecules into one macromolecule. The reinforced interactions between the molecules induce the formation of molecular self-assembly with not only highly ordered structure but also large dimensions. A porphyrin ring covalently connected with four PDI units has been prepared by Wasielewski and co-

* To whom correspondence should be addressed. E-mail: xiyouli@sdu.edu.cn.

† Shandong University.

‡ College of Shandong Police.

(1) Law, K.-Y. *Chem. Rev.* **1993**, *93*, 449–486.
(2) Gregg, B. A. *J. Phys. Chem. B* **2003**, *107*, 4688–4698.
(3) Cormier, R. A.; Gregg, B. A. *Chem. Mater.* **1998**, *10*, 1309–1319.
(4) Gosztola, D.; Niemczyk, M. P.; Wasielewski, M. R. *J. Am. Chem. Soc.* **1998**, *120*, 5118–5119.
(5) Zhao, Y.; Wasielewski, M. R. *Tetrahedron Lett.* **1999**, *40*, 7047–7050.
(6) Hayes, R. T.; Wasielewski, M. R.; Gosztola, D. *J. Am. Chem. Soc.* **2000**, *122*, 5563–5567.
(7) Just, E. M.; Wasielewski, M. R. *Superlattices Microstruct.* **2000**, *28*, 317–328.
(8) Miller, S. E.; Zhao, Y.; Schaller, R.; Mulloni, V.; Just, E. M.; Johnson, R. C.; Wasielewski, M. R. *Chem. Phys.* **2002**, *275*, 167–183.
(9) Lukas, A. S.; Zhao, Y.; Miller, S. E.; Wasielewski, M. R. *J. Phys. Chem. B* **2002**, *106*, 1299–1306.
(10) Giaimo, J. M.; Gusev, A. V.; Wasielewski, M. R. *J. Am. Chem. Soc.* **2002**, *124*, 8530–8531.
(11) Van der Boom, T.; Hayes, R. T.; Zhao, Y.; Bushard, P. J.; Weiss, E. A.; Wasielewski, M. R. *J. Am. Chem. Soc.* **2002**, *124*, 9582–9590.
(12) Ahrena, M. J.; Fuller, M. J.; Wasielewski, M. R. *Chem. Mater.* **2003**, *15*, 2684–2686.
(13) Andersson, M.; Sinks, L. E.; Hayes, R. T.; Zhao, Y.; Wasielewski, M. R. *Angew. Chem., Int. Ed.* **2003**, *42*, 3139–3143.
(14) Liu, S.-G.; Sui, G.; Cormier, R. A.; Leblanc, R. M.; Gregg, B. A. *J. Phys. Chem. B* **2002**, *106*, 1307–1315.
(15) Struijk, C. W.; Sieval, A. B.; Dakhorst, J. E. J.; van Dijk, M.; Kimkes, P.; Koehorst, R. B. M.; Donker, H.; Schaafsma, T. J.; Picken, S. J.; van de Craats, A. M.; Warman, J. M.; Zuilhof, H.; Sudhölter, E. J. R. *J. Am. Chem. Soc.* **2000**, *122*, 11057–11066.
(16) Wang, W.; Han, J. J.; Wang, L.-Q.; Li, L.-S.; Shaw, W. J.; Li, A. D. Q. *Nano Lett.* **2003**, *3*, 455–458.
(17) Wang, W.; Li, L.-S.; Helms, G.; Zhou, H.-H.; Li, A. D. Q. *J. Am. Chem. Soc.* **2003**, *125*, 1120–1121.
(18) Würthner, F.; Thalacker, C.; Sautter, A.; Schärtl, W.; Ibach, W.; Hollricher, O. *Chem.—Eur. J.* **2000**, *6*, 3871–3886.
(19) Würthner, F.; Thalacker, C.; Diele, S.; Tschierske, C. *Chem.—Eur. J.* **2001**, *7*, 2245–2253.
(20) Würthner, F.; Chen, Z.; Hoeben, F. J. M.; Osswald, P.; You, C.-C.; Jonkheijm, P.; Herrikhuyzen, J. V.; Schenning, A. P. H. J.; van der Schoot, P. P. A. M.; Meijer, E. W.; Beckers, E. H. A.; Meskers, S. C. J.; Janssen, R. A. J. *J. Am. Chem. Soc.* **2004**, *126*, 10611–10618.
(21) Würthner, F. *Chem. Commun.* **2004**, 1564–1579.
(22) Iverson, I. K.; Casey, S. M.; Seo, W.; Tam-Chang, S.-W.; Pindzola, B. A. *Langmuir* **2002**, *18*, 3510–3516.
(23) Neuteboom, E. E.; Meskers, S. C. J.; Meijer, E. W.; Janssen, R. A. *J. Macromol. Chem. Phys.* **2004**, *205*, 217–222.
(24) Ahrens, M. J.; Sinks, L. E.; Rybtchinski, B.; Liu, W.; Jones, B. A.; Giaimo, J. M.; Gusev, A. V.; Goshe, A. J.; Tiede, D. M.; Wasielewski, M. R. *J. Am. Chem. Soc.* **2004**, *126*, 8284–8294.
(25) Hernando, J.; de Witte, P. A. J.; van Dijk, E. M. H. P.; Korterik, J.; Nolte, R. J. M.; Rowan, A. E.; García-Parajó, M. F.; van Hulst, N. F. *Angew. Chem., Int. Ed.* **2004**, *43*, 4045–4049.
(26) Van Gorp, J. J.; Vekemans, J. A. J. M.; Meijer, E. W. *J. Am. Chem. Soc.* **2002**, *124*, 14759–14769.
(27) Wang, Y.; Chen, Y.; Li, R.; Wang, S.; Su, W; Ma, P.; Wasielewski, M. R.; Li, X.; Jiang, J. *Langmuir* **2007**, *23*, 5836–5842.
(28) Würthner, F.; Stepanenko, V.; Chen, Z.-J.; Saha-Möller, C. R.; Kocher, N.; Stalke, D. *J. Org. Chem.* **2004**, *69*, 7933–7939.
(29) Jonkheijm, P.; Stutzmann, N.; Chen, Z.-J.; de Leeuw, D. M.; Meijer, E. W.; Schenning, A. P. H. J.; Würthner, F. *J. Am. Chem. Soc.* **2006**, *128*, 9535–9540.
(30) Chen, Z.-J.; Baumeister, U.; Tschierske, C.; Würthner, F. *Chem.—Eur. J.* **2007**, *13*, 450–465.
(31) Yagai, S.; Seki, T.; Karatsu, T.; Kitamura, A.; Würthner, F. *Angew. Chem., Int. Ed.* **2008**, *47*, 3367–3371.
(32) Kaiser, T. E.; Wang, H.; Stepanenko, V.; Würthner, F. *Angew. Chem.* **2007**, *119*, 5637–5640.
(33) Che, Y.; Datar, A.; Balakrishnan, K.; and Zang, L. *J. Am. Chem. Soc.* **2007**, *129*, 7234–7235.
(34) Dehm, V.; Chen, Z.-J.; Baumeiste, U.; Prins, P.; Siebbeles, L. D. A.; Würthner, F. *Org. Lett.* **2007**, *9*, 1085–1088.

10.1021/la801463u CCC: $40.75
Published on Web 08/27/2008

Scheme 1. Molecular Structure of PDI Trimers 1−3 and Monomers 1−3

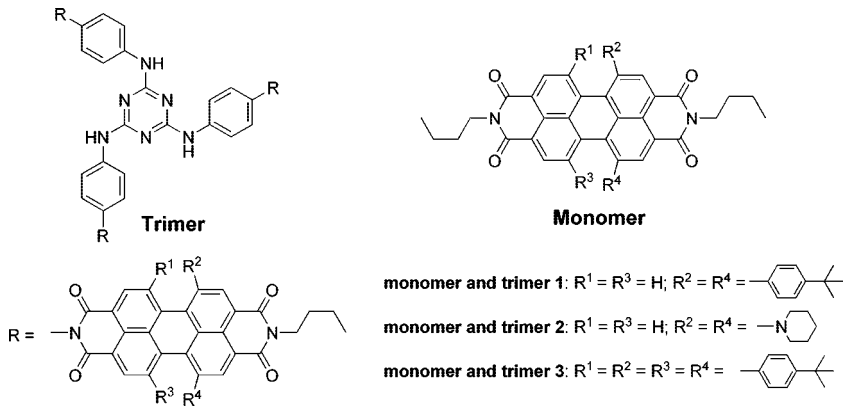

workers, and the aggregation of this compound in solution and solid films has been studied by electronic absorption and emission spectra together with atomic force microscopy (AFM).[11] From the same group, molecules with four or five PDI units connected by covalent bonds were reported.[24] Solution X-ray scattering experiments revealed the formation of stable aggregates in nonpolar solvents. The coplanar conformation of these PDI units has reinforced the $\pi-\pi$ interactions between the molecules and induces the formation of large aggregates in solution with high stability. A phthalocyanine appended with four PDI units at peripheral positions can form a heptamer in nonpolar solvents with a well-defined face-to-face stacked structure.[35,36] Quick, efficient energy transfer between the aggregated PDIs and phthalocyanines was observed. A hexaazatriphenylene appended with six PDI units was self-assembled in both solution and solid films to form a highly stabilized dimeric aggregate in which efficient energy transfer from the hexaazatriphenylene core to the PDI moieties occurs.[37] Moreover, three PDI units connected by a rigid 1,3,5-triphenyl benzene group form a propellerlike PDI trimer. This trimer self-aggregated into 1D nanofibers with very large aspect ratios.[38] Polarized scanning confocal microscopy revealed that the plan of PDI rings is perpendicular to the axis of the fibers and suggested that these fibers maybe useful in nanoscale devices, such as field-effect transistors and photoconductors. The work mentioned above is based on molecules with rigid molecular structure. The PDI units of these molecules are forced to form a coplanar conformation by the linkage. Although PDI oligomers, such as hexamers and tetramers, connected by flexible linkages have been prepared by Langhal and co-workers,[39] the aggregation behavior of these molecules both in solution and the solid state is not known.

Here we present the design and synthesis of a series of novel PDI trimers connected by a triazine ring (Scheme 1). They are different from those connected by the rigid 1,3,5-triphenyl benzene group because the PDI units in these compounds can rotate freely along the C−N−C bonds between the phenyl groups and the triazine ring, which will bring some flexibility to the molecules. Different groups have been introduced into the bay positions of the PDI rings, which are expected to introduce different steric hindrance to the molecule. The phenylene linkers between the central triazine and three perylene diimide subunits are helpful for keeping the coplanar conformation of the PDI subunits. The branched structure together with the coplanar conformation is expected to reinforce the $\pi-\pi$ interactions between the molecules and thus improve the structure of the nano self-assembly.

Results and Discussion

Synthesis. The title compounds were prepared following the procedures shown in Supporting Information scheme S1. The linkage, 1,3,5-tri(4′-aminophenyl)amino-2,4,6-triazine (**6**), was prepared by the nucleophilic substitution of 1,3,5-trichloride-2,4,6-traizine and *p*-nitroaniline, which is followed by a reduction of the nitro groups by $SnCl_2$. We have tried to prepare **6** with a one-step reaction of 1,3,5-trichloride-2,4,6-traizine with excess 1,4-diaminobenzene, but the production yield is extremely low and is accompanied by very difficult separation and purification procedures. On the contrary, the yield of the two-step method is high, and the workup procedures are simple. Condensations of **6** with different monoanhydrides (1,7-di(4′-*tert*-butyl)phenoxy-perylene-9,10-(*N*-butyl)-dicarboxyimide-3,4-dicarboxylic anhydride **7**, *N*-*n*-butyl-1,7-dipiperidinylperylene-3,4:9,10-tetracarboxylic acid-3,4-anhydrid- 9,10-imide **8**, and *N*-*n*-butyl-1,6,7,12-tetra(4-*tert*-butylphenoxy)perylene-3,4:9,10-tetracarboxylic-3,4-anhydride-9,10-imide **9**) in refluxing toluene and imidazole give the corresponding PDI trimers in yields of 58, 52, and 47% for trimers **1**−**3**, respectively. Other methods such as condensation in refluxing pyridine and DMF can also give the products, but with lower yields. All of the PDI trimers show very good solubility in conventional halogenated organic solvents, such as dichloromethane and chloroform, but with small solubility in alcoholic solvents such as methanol and ethanol. This provides the possibility to use mixed solvents of chloroform and methanol to prepare the self-assembly of these compounds. For comparison purposes, three PDI monomers have also been prepared following the literature methods (Scheme 1).

UV−Vis Absorption Spectroscopy. UV−vis absorption spectra of PDIs are sensitive to the interchromophore distance and orientation[40] and therefore have been widely used to study their $\pi-\pi$ stacking.[17,41,42] Figure 1A shows the absorption spectra of trimer **1** in a mixed solvent of 1:9 MeOH/$CHCl_3$ at different concentrations. At low concentration (1×10^{-7} mol L^{-1}), the spectra of trimer **1** show two peaks at 550 and 515 nm, which correspond to the 0−0 and 0−1 transitions, respectively.[33] The

(35) Li, X.; Sinks, L. E.; Rybtchinski, B.; Wasielewski, M. R. *J. Am. Chem. Soc.* **2004**, *126*, 10810–10811.
(36) Wasielewski, M. R. *J. Org. Chem.* **2006**, *71*, 5051–5066.
(37) Ishi-I, T.; Murakami, K.; Imai, Y.; Mataka, S. *Org. Lett.* **2005**, *7*, 3175–3178.
(38) Yan, P; Chowdhury, A.; Holman, M. W.; Adams, D. M. *J. Phys. Chem. B* **2005**, *109*, 724–730.
(39) Langhal, H. *Helv. Chim. Acta* **2005**, *88*, 1309–1343.
(40) Kazmaier, P. M.; Hoffmann, R. *J. Am. Chem. Soc.* **1994**, *116*, 9684–9691.
(41) Balakrishnan, K.; Datar, A.; Oitker, R.; Chen, H.; Zuo, J.; Zang, L. *J. Am. Chem. Soc.* **2005**, *127*, 10496–10497.
(42) Balakrishnan, K.; Datar, A.; Naddo, T.; Huang, J.; Oitker, R.; Yen, M.; Zhao, J.; Zang, L. *J. Am. Chem. Soc.* **2006**, *128*, 7390–7398.

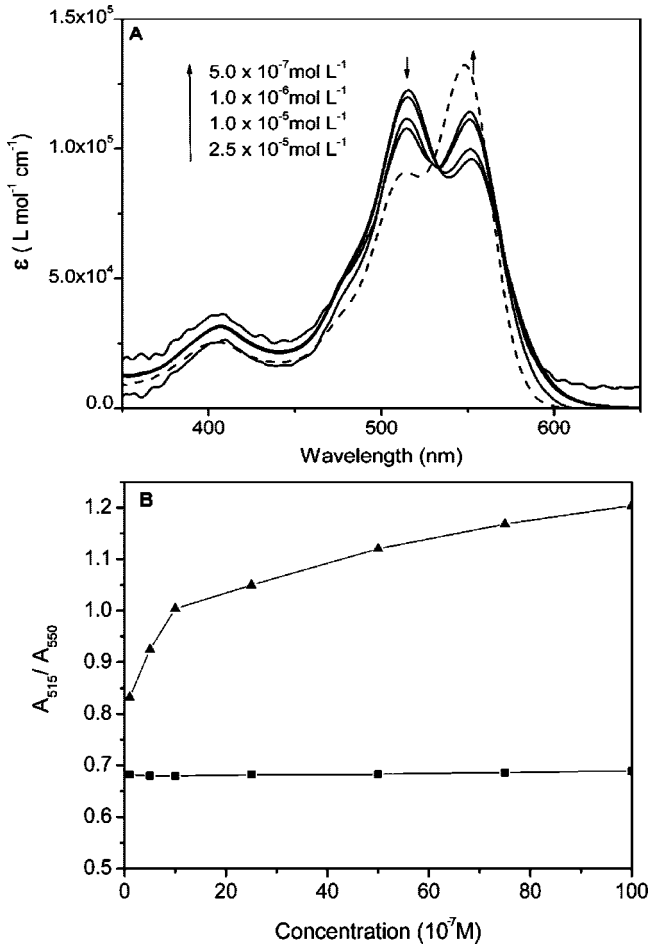

Figure 1. (A) Concentration-dependent absorption spectra of trimer **1** in 1:9 MeOH/$CHCl_3$ (−) compared with the normalized absorption spectra of monomer **1** (multiplied by 3) in the same solvent (---). (B) Plot of A_{515}/A_{550} in the absorption spectra of trimer **1** (▲) or monomer **1** (□) vs concentration.

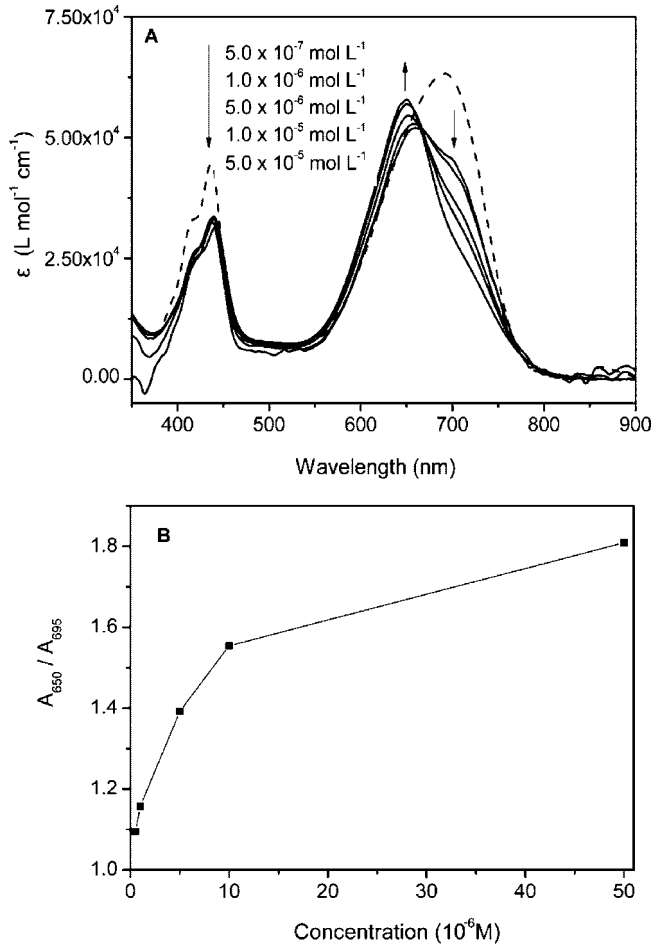

Figure 2. (A) Concentration-dependent absorption spectra of trimer **2** in 1:9 MeOH/$CHCl_3$ (−) compared with the normalized absorption spectra of monomer **2** (multiplied by 3) in the same solvent (---). (B) Plot of A_{650}/A_{695} in the absorption spectra of trimer **2** vs concentration.

intensity of the peak at 550 nm is a little bit larger than that of the peak at 515 nm. Following the previous report, the 0−0 and 0−1 transitions will reverse in intensity upon $\pi-\pi$ stacking.[43] Therefore, the intensity ratio of the peaks at 515 and 550 nm is directly correlated with the proportion of aggregates against monomer in solution. Figure 1B show the plots of the intensity ratio between the absorption peaks at 515 and 550 nm (A_{515}/A_{550}) of trimer **1** and monomer **1** against concentration. In the concentration range of $10^{-8}-10^{-6}$ mol L^{-1}, the A_{515}/A_{550} ratio of monomer **1** remains almost unchanged, suggesting no intermolecular aggregation at this concentration. However, the A_{515}/A_{550} ratios of trimer **1** in the same concentration range are significantly larger than that of the corresponding monomer **1** and increase significantly along with the concentration increase, which indicates the presence of aggregations of PDI in such a dilute solution. This result suggests that trimer **1** forms self-aggregates more easily than monomer **1** and the connecting of three PDI units into one molecule has indeed synergically reinforced the interactions between molecules.

Two obviously different stages were observed in the curve of A_{515}/A_{550} versus the concentration of trimer **1**. In the low-concentration range (i.e., smaller than 1×10^{-6} mol L^{-1}), the A_{515}/A_{550} ratio increase sharply along with the increase in concentration, but when the concentration of trimer **1** is larger than 1×10^{-6} mol L^{-1}, A_{515}/A_{550} increases linearly with a smaller slope along with the concentration increase. This result suggests the presence of equilibrium between the aggregates and non-aggregates in the concentrated solution.

The absorption spectra of monomer **2** show the maxima absorption band at 695 nm, which is not concentration-dependent in the range of $10^{-5}-10^{-7}$ mol L^{-1}. However, the absorption spectra of trimer **2** (Figure 2) present a blue-shifted absorption peak at 660 nm with a large concentration dependence. In dilute solution, the spectra show one peak at about 660 nm with a shoulder at 695 nm. This blue-shifted absorption peak relative to its monomeric counterpart suggests the presence of the face-to-face stacked dimeric structure of PDIs in the diluted solution of trimer **2**,[10] which is similar with that of trimer **1**. With the increase in concentration from 5×10^{-7} to 2.5×10^{-5} mol L^{-1}, the shoulder at 695 nm disappeared gradually, accompanied by a significant increase in the peak at 660 nm, indicating the steady increase in the concentration of face-to-face stacked aggregates in the solution. It is worth noting that the PDIs with nitrogen substitution at 1,7 positions cannot form a face-to-face stacked structure in solution because of the large steric hindrance brought about by the side groups.[44] The one and only example of the H aggregates of PDI with nitrogen substitution at 1,7 positions is presented by a PDI dimer linked by a rigid xanthene spacer in

(43) Clark, A. E.; Qin, C.; Li, A. D. Q. *J. Am. Chem. Soc.* **2007**, *129*, 7586–7595.

(44) Su, W.; Zhang, Y.; Zhao, C.; Li, X.; Jiang, J. *ChemPhysChem* **2007**, *8*, 1857–1862.

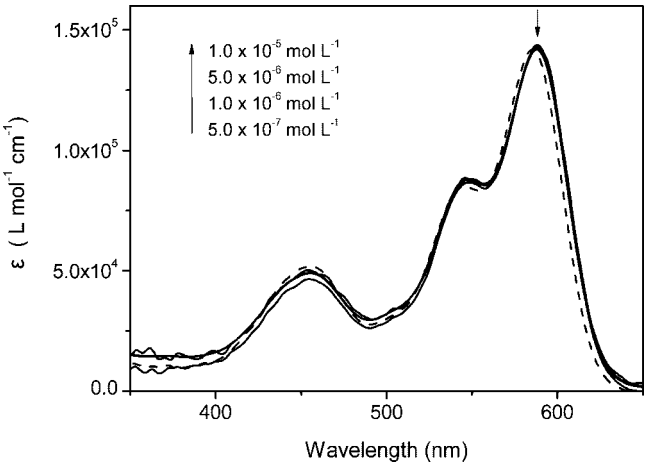

Figure 3. Concentration-dependent absorption spectra of trimer **3** in 1:9 MeOH/$CHCl_3$ (−) compared with the normalized absorption spectra of monomer **3** (multiplied by 3) in the same solvent (---).

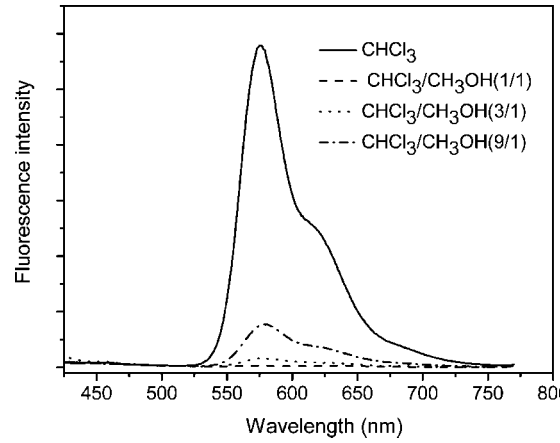

Figure 4. Fluorescence spectra of trimer **1** in $CHCl_3$ with different contents of CH_3OH (λ_{ex} = 400 nm, the absorption at the excitation wavelength was normalized).

which the PDI units were forced to take a face-to-face conformation.[10] The formation of H aggregates of PDIs in trimer **2** revealed the significantly reinforced $\pi-\pi$ interactions between the molecules of trimer **2**.

Similar to that of trimer **1**, the changes in A_{650}/A_{695} against the concentration of trimer **2** as shown in Figure 2B can also be divided into two stages. In the first stage, corresponding to the concentration range of 5×10^{-7} to 1.0×10^{-5} mol L^{-1}, the A_{650}/A_{695} ratio increase sharply along with the concentration increase, but in the second stage, when the concentration of trimer **2** is lager than 1.0×10^{-5} mol L^{-1}, the A_{650}/A_{695} ratio increase smoothly along with the concentration increase, which indicates the achievement of equilibrium between aggregates and nonaggregates. It is worth noting that the similar equilibrium between the aggregates and nonaggregates for trimer **1** was built at 1×10^{-6} mol L^{-1}, which is significantly smaller than that of trimer **2**, suggesting that trimer **1** forms aggregates more easily than does the latter.

Contrary to that of trimers **1** and **2**, the absorption spectra of trimer **3** do not change significantly along with the concentration increase (Figure 3). A small red shift (4 nm) on the absorption peak was observed for trimer **3** relative to that of monomer **3**, which can be attributed to the formation of *J* aggregates as reported previously. This result suggests that the large steric hindrance of the substitute at bay positions has induced the formation of *J* aggregates but efficiently hindered the formation of *H* aggregates. This is in accordance with the results of the other systems based on the PDIs.[20,45]

To evaluate the aggregation behavior of these three compounds quantitatively, the binding constants of the aggregates, K_{agg}, were calculated on the basis of an isodesmic or equal-*K* model, which assumes equal binding constants for all binding events to a 1D columnar aggregate of equal components independently of the size of the aggregates and has been applied successfully to the stacking of aromatic compounds in solution.[45] K_{agg} calculated for trimer **1** is 4.36×10^5 mol^{-1} L, which is significantly larger than that of trimer **2** (5.12×10^4 mol^{-1} L). However, the calculation of K_{agg} for trimer **3** does not give a reasonable result probably because of the serious departure of the model used in the calculation from the actual aggregation mechanisms of trimer **3** in solution. The K_{agg} values calculated for monomeric models **7** and **8** are 341 and 182 mol^{-1} L, respectively, which are significantly smaller than those of trimers **1** and **2** and clearly show the significant synergistic effect of PDI units in trimers on the reinforcement of the intermolecular interactions.

Fluorescence Spectra. $\pi-\pi$ stacking of PDIs always induces red-shifted emission, which is usually attributed to the excimer's emission, with low fluorescence quantum yields.[46] Therefore, the fluorescence spectra measurement is another powerful tool for the investigation of PDI self-aggregation in addition to the UV−vis absorption spectra. The fluorescence spectra of trimer **1** in chloroform with different contents of methanol are shown in Figure 4. The fluorescence quantum yields are calculated with monomer **1** (quantum yield 100%) as a standard, and the results are listed in Table 1.

In pure chloroform, trimer **1** shows strong emission at 575 nm with a fluorescence quantum yield of 40.2%. The lower fluorescence quantum yield relative to that of monomer **1** can be ascribed to the aggregation of trimer **1** in chloroform.[27] When methanol was added to the solution, the fluorescence of trimer **1** was further remarkably quenched as a result of the formation of intermolecular aggregates induced by the decreased solubility of trimer **1** in the mixed solvents. The plot of fluorescence quantum yields of trimer **1** against the content of CH_3OH in $CHCl_3$ (Figure 5) shows clearly that the intermolecular aggregation of trimer **1** happened in a very small content of methanol in chloroform.

The fluorescence spectra of trimer **2** in chloroform are similar in shape to that of monomer **2**. Both of them show very small fluorescence quantum yields because of the partial electron transfer from piperidine to the PDI core.[10,47] Although the fluorescence quantum yield of trimer **2** is generally smaller than that of monomer **2** in pure chloroform or the mixed solvents of $CHCl_3/CH_3OH$, we cannot attribute the fluorescence quenching directly to the aggregation because the reinforced partial electron transfer between piperidine and PDI in more polar solvents will also induce significant fluorescence quenching.

The fluorescence spectra of trimer **3** in mixed solvents of chloroform and methanol with different contents of methanol show similar fluorescence quenching to that of trimer **1**. The fluorescence quantum yields decrease significantly along with the increase in the content of methanol in the mixed solvents, suggesting the formation of aggregates in the mixed solvents (Figure 5). However, the plot of fluorescence quantum yields

(45) Martin, R. B. *Chem. Rev.* **1996**, *96*, 3043–3064.

(46) Giaimo, J. M.; Lockard, J. V.; Sinks, L. E.; Scott, A. M.; Wilson, T. M.; Wasielewski, M. R. *J. Phys. Chem. A* **2008**, *112*, 2322–2330.

(47) Zhao, C.; Zhang, Y.; Li, R.; Li, X.; Jiang, J. *J. Org. Chem.* **2007**, *72*, 2402–2410.

Table 1. Fluorescence Quantum Yields of Trimers 1−3 and Monomer 1−3 at 1×10^{-6} mol L^{-1} in $CHCl_3$ with Different Contents of CH_3OH

	Φ_f (%)					
content (%) of CH_3OH in $CHCl_3$	trimer **1**	trimer **2**	trimer **3**	monomer **1**	monomer **2**	monomer **3**
0	40.2	1.1	79.5	100	2.2	82.6
5	20.1	0.8	59.2	97.5	2.1	82.0
10	9.1	0.5	41.2	95.6	1.9	81.5
15	4.0	0.3	24.9	95.5	1.8	81.0
20	2.6	0.1	16.8	95.0	1.7	80.5
25	1.0	0.06	9.3	94.0	1.6	80.1
50	0.1	0	1.4	93.0	1.4	79.2

against the content of methanol in chloroform indicates that the fluorescence quantum yields of trimer **3** are less sensitive to methanol content than that of timer **1**. The result of the fluorescence spectra seems to conflict with the results of UV−vis absorption spectra because the latter suggest no or small aggregation of trimer **3** in solution. This discrepancy might be caused by the different sensitivity of absorption and fluorescence spectra. Fluorescence spectra are much more sensitive to aggregation than absorption spectra. A small portion of aggregation of trimer **3** in solution will induce a larger amount of fluorescence quenching.

Morphologies of the Aggregates. In a typical experiment, a solution of trimer **1** (50 μM) in 9:1 CH_2Cl_2/MeOH is allowed to evaporate slowly, and the preferential evaporation of CH_2Cl_2 (bp 40 °C) over MeOH (bp 64.7 °C) gradually lowers the solubility and favors self-organization into thermodynamically stable structures. The aggregates formed were transferred to the substrates (glass slides or single-crystal silicon) by simply immersing the substrate in the solution as it evaporated. The morphology of the nanoaggregates was recorded by atomic force microscopy (AFM) via the tapping model.

Figure 6A shows the morphology of the nanoaggregates of trimer **1**. Nanofibers with a very large aspect ratio were formed by trimer **1**. The diameters of the fibers are in the range of 30−230 nm, and the length can reach up to tens of micrometers. These fibers can also be found on a surface patterned with silicon (Figure 6B). No abrupt change in the direction or diameter of the fibers is observed at the glass and silicon boundary, indicating that the fibers self-organize in solution and then precipitate onto the surface.[38] The morphology of the aggregates is not essentially affected by the initial concentration of trimer **1** but is sensitive to the component of the solvents. A large initial concentration of trimer **1** results in no changes in the shape of the aggregates, but a pure dichloromethane solution of trimer **1** results in spherical nanoparticles only. With the same method, trimers **2** and **3** can form only sphere nanoparticles as shown in Figure 6C,D. Different initial concentrations and solvent components are tried, but no fibers can be obtained for these two trimers. This result is obviously correlated with the substituents at bay positions of the PDIs. As revealed by the UV−vis absorption and fluorescence spectra, trimers **2** and **3** show weaker intermolecular interactions because of the larger steric hindrance. The reduced intermolecular interactions hindered the molecular aggregate in one direction to form long fibers.

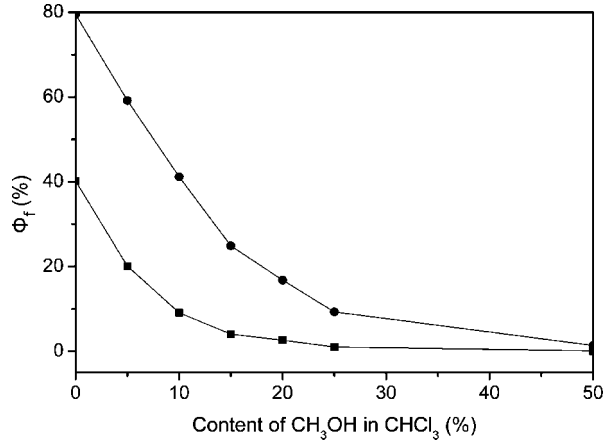

Figure 5. Plot of fluorescence quantum yield of trimers **1** (■) and **3** (●) vs the content of CH_3OH in $CHCl_3$.

XRD Experiments. The structures of the nanoaggregates were further investigated by X-ray diffraction (XRD) techniques. Figure 7 shows the diffraction patterns of the self-assembled nanostructures of trimers **1**−**3**. Two diffraction peaks were observed in the low-angle region for the diffraction pattern of trimer **1**, indicating the highly ordered structure of the nanofibers. The most significant diffraction peak appeared at $2\theta = 1.33°$, which was accompanied by another minor peak at $2\theta = 1.85°$. The d spacings calculated from the Bragg equation according to the 2θ values are about 6.6 and 4.8 nm. The smaller d spacing can be ascribed to the length of the molecules as shown in Figure 8A,B, and the larger d spacing is attributed to the length of the dimeric aggregates of two trimer **1** molecules connected by a pair of

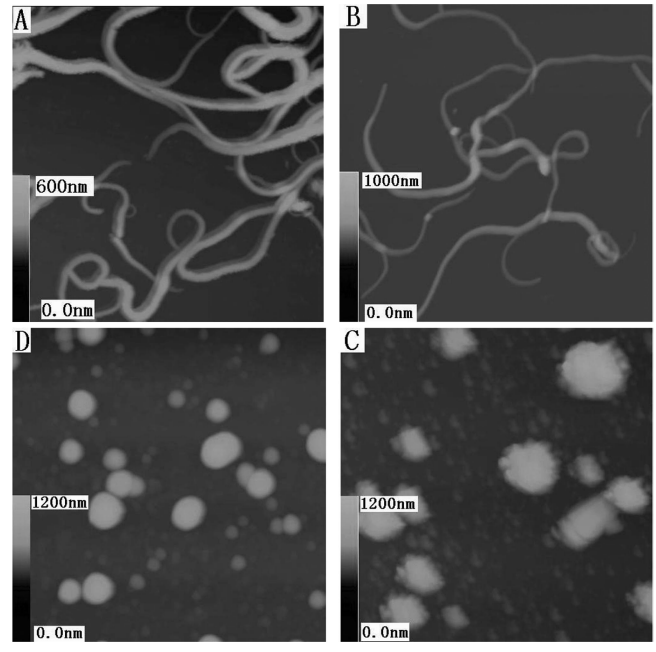

Figure 6. (A) AFM image (10 μm × 10 μm) of trimer **1** nanofibers on a glass surface. (B) AFM image (10 μm × 10 μm) of trimer **1** nanofibers on a silicon surface. (C) AFM image (10 μm × 10 μm) of trimer **2** nanofibers on a glass surface. (D) AFM image (10 μm × 10 μm) of trimer **3** nanofibers on a glass surface.

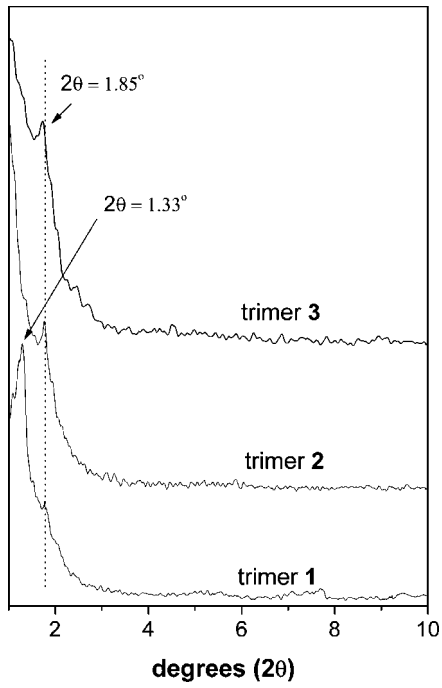

Figure 7. XRD profiles of the aggregates of trimers **1**−**3**.

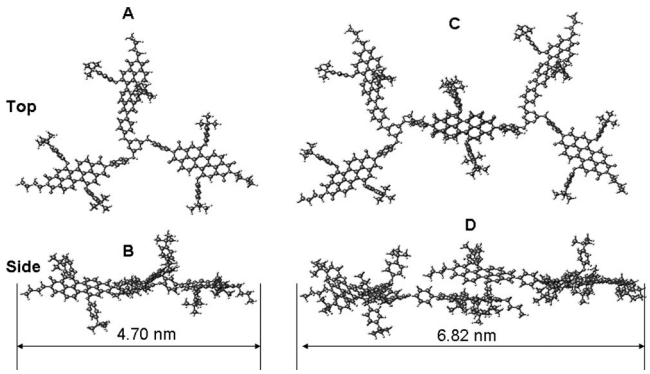

Figure 8. Energy-minimized molecular structure of trimer **1** (A and B) and its dimeric aggregates (C and D).

overlapping PDI units that belong to different molecules (Figure 8C,D).

The X-ray diffraction patterns of trimers **2** and **3** are similar (Figure 8A,B). Both of them show one diffraction peak at about $2\theta = 1.85°$ in the low-angle region that can be assigned similarly to the length of the molecule. However, the peak at $2\theta = 1.33$, which is present in the diffraction profile of timer **1**, disappeared from the profiles of trimers **2** and **3**. This suggests that the dimeric aggregates of trimers **2** and **3** are not the dominating periodic structure unit in the nanoaggregates, probably because of the weak interaction between the PDIs as also supported by the UV−vis absorption and fluorescence spectra.

In conclusion, three novel PDI trimers with some flexibility in the molecular structure were prepared and characterized. A simple evaporation method was used for the preparation of the nanoaggregates of these trimers in the solid state. Despite the flexible molecular structure, the 3-fold branched structure of the trimers has reinforced the interactions between the trimer molecules significantly as compared with those of their monomeric counterparts. The strong interactions between the trimer molecules have driven the formation of aggregates of trimer molecules in extremely dilute solutions. The steric hindrance introduced by the substituents at bay positions affects the aggregation behavior efficiently. Molecules with small steric hindrance favor face-to-face $\pi-\pi$ stacking and the formation of nanofibers with highly ordered structure whereas the molecules with large steric hindrance self-aggregate into nanoparticles with spherical morphology only. We believe that these results will be helpful in guiding the fabrication of organic functional materials into nanostructures for molecular electronic devices using molecular design and synthesis.

Experimental Section

General Methods. ^{1}H NMR spectra were recorded at 300 MHz with the solvent peak as the internal standard (in $CDCl_3$). Electronic absorption spectra were recorded on a Hitachi 4100 spectrometer. Fluorescence spectra were measured on an ISS K2 system. The fluorescence quantum yields are calculated with monomer **1** as a standard. MALDI-TOF mass spectra were taken on an ultrahigh-resolution Fourier transform ion cyclotron resonance (FT-ICR) mass spectrometer. The morphology of nanostructures on Si or glass was studied in air by use of a Veeco multimode atomic force microscope (AFM) in tapping mode. The low-angle X-ray diffraction (LAXD) experiment was carried out on a Rigaku D/max-γB X-ray diffractometer.

The binding constants, K_{agg}, in 1:9 $CH_3OH/CHCl_3$ of trimers **1**−**3** were calculated on the basis of an isodesmic or equal-K_{agg} model. A set of spectra of trimers **1**−**3** at different concentrations in 1:9 $CH_3OH/CHCl_3$ were recorded. The apparent extinction coefficients at several wavelengths were fitted by nonlinear regression according to eq 1, derived from ref 45

$$\varepsilon(c) = \frac{2Kc + 1 - \sqrt{4Kc + 1}}{2K^2c^2}(\varepsilon_f - \varepsilon_a) + \varepsilon_a \qquad (1)$$

ε denotes the apparent extinction coefficient obtained from the spectra; ε_f and ε_a are the extinction coefficients for the free and aggregated species, respectively; K is the binding constant; and c is the total dye concentration in the sample.

Synthesis. Column chromatography was carried out on silica gel (Merck, Kieselgel 60, 70−230 mesh) with the indicated eluents. All other reagents and solvents were used as received without further purification.

2,4,6-Tris(*p*-nitroanilino)-1,3,5-triazine (5). Cyanuric chloride (2.31 g, 12.5 mmol), *p*-nitroaniline (8.65 g, 62.5 mmol), and K_2CO_3 (10.4 g, 75mmol) were mixed in 120 mL of 1,4-dioxane. The mixture was refluxed for 24 h, and then the solid product was separated from the reaction mixture by filtration. After being washed successively with water (100 mL × 3), methanol (50 mL × 3), and benzene (50 mL × 3), the solid was dried under reduced pressure overnight. **5** was collected as a white solid (5.12 g, yield: 84.4%); mp > 300 °C; ^{1}H NMR (300 MHz, DMSO-d_6): δ 10.33 (s, 3H), 8.25 (d, J = 9.1 Hz, 6H), 8.16 (d, J = 9.1 Hz, 6H); MALDI-TOF MS (*m*/*z*) 489, calcd for $C_{21}H_{15}N_9O_6$ (*m*/*z*) 489. Anal. Calcd for $C_{21}H_{15}N_9O_6$: C, 51.54%; H, 3.09%; N, 25.76%. Found: C, 51.23%; H, 3.12%; N, 25.46%.

2,4,6-Tris(*p*-aminoanilino)-1,3,5-triazine (6). To a solution of **5** (4.89 g, 10.0 mmol) in ethanol (20 mL) was added a mixture of HCl (36%, 30 mL) and $SnCl_2 \cdot 2H_2O$ (20.7 g, 91.5 mmol) in ethanol (30 mL) at room temperature in 1 h. After 48 h of reflux, the precipitate in the reaction mixture was separated by filtration. The separated solid was redissolved in hot water; the insoluble byproducts were separated by filtration. The filtrate was neutralized in a NaOH aqueous solution until pH ≥ 11 was reached. The solid product was collected by filtration and washed successively with water (100 mL × 3) and methanol. After being dried under reduced pressure overnight, **6** was collected as a pale-yellow solid (1.03 g, yield 26.2%); mp 286 °C; ^{1}H NMR (300 MHz, DMSO-d_6): δ 8.52 (s, 3H), 7.35 (bs, 6H), 6.53(bs, 6H), 4.72 (s, 6H); MALDI-TOF MS (*m*/*z*) 399, calcd for $C_{21}H_{21}N_9$ (*m*/*z*) 399. Anal. Calcd for $C_{21}H_{21}N_9$: C, 63.14%; H, 5.30%; N, 31.56%. Found: C, 63.25%; H, 5.43%; N, 30.98%.

1,7-Di(4′-tert-butyl)phenoxy-perylene-9,10-(N-butyl)-dicarboxyimide-3,4-dicarboxylic anhydride (7). A solution of 1,7-Di(4′-*tert*-butyl)-phenoxy-perylene-3,4;9,10-tetracarboxy dianhydride[11] (1.4 g, 2.0 mmol) in pyridine (100 mL) was purged with dry nitrogen for 15min and then was heated to reflux. To this solution *n*-butylamine (146 mg, 2 mmol) in pyridine (10 mL) was added slowly over the course of 30 min. The resulting mixture was refluxed continuously for another 30 min, and then the volatiles were removed under reduced pressure. The residue was purified by column chromatography on silica gel with chloroform as eluent. Repeated chromatography followed by recrystallization from a mixture of $CHCl_3$ and MeOH gave pure **7** as red solid (782 mg, yield 53%): mp. > 300 °C; ^{1}H NMR ($CDCl_3$, 300 MHz) δ 9.64 (d, J = 8.4 Hz, 2H), 8.58−8.62 (d+d, J = 8.4 Hz, 2H), 8.35(s+s, 2H), 7.52 (m, 4H), 7.14 (m, 4H), 4.15 (t, J = 7.2 Hz, 2H), 1.63 (br, 2H), 1.40 (s, 18H), 1.27 (br, 2H), 0.90 (br, 3H); MALDI-TOF MS(*m*/*z*) 744.7, calcd for $C_{48}H_{41}NO_7$(*m*/*z*) 743.8. Anal. Calcd for $C_{48}H_{41}NO_7$: C, 77.50; H, 5.56; N, 1.88. Found: C, 77.42; H, 5.65; N, 2.03.

***N*-*n*-Butyl-1,7-dipiperidinylperylene-3,4:9,10-tetracarboxylic acid-3,4-anhydride-9,10-imide (8).** A mixture of *N*,*N*′-dibutyl-1,7-dipiperidinylperylene-3,4:9,10- tetracarboxylic diimide (250.0 mg, 0.36 mmol),[5,48] KOH (1 g, 18 mmol) in 2.5 mL of water, and 15 mL of *tert*-butyl alcohol was brought to reflux. The mixture was stirred at reflux for 3 h and poured under stirring into 50 mL of AcOH. The green product was extracted from the acetic acid with methylene chloride (50 mL × 3). The combined organic phase was washed with water, dried over $MgSO_4$, and concentrated by rotary evaporation. Column chromatography on silica gel with 10:1:9 chloroform/acetone/hexane as the eluent afforded product **8** (62 mg, 27%); mp 214 °C; ^{1}H NMR ($CDCl_3$, 300 MHz): δ 9.53 (d, J = 8.22 Hz, 1H), 9.42 (d, J = 8.26 Hz, 1H), 8.42 (s, 1H), 8.40 (s, 1H), 8.38 (d, J = 2.09 Hz, 1H), 8.36 (d, J = 1.97 Hz, 1H), 4.22 (m, 2H), 3.47 (m, 4H), 2.90 (m, 4H), 1.40−1.70 (m,16H), 1.00−1.50 (t, 3H); MALDI-TOF MS(*m*/*z*) 614.7, calcd for $C_{38}H_{35}N_3O_5$ (*m*/*z*) 613.7. Anal. Calcd for $C_{38}H_{35}N_3O_5$: C, 74.37; H, 5.75; N, 6.85. Found: C, 74.53; H, 5.67; N, 6.79.

***N*-*n*-Butyl-1,6,7,12-tetra(4-tert-butylphenoxy)perylene-3,4:9,10-tetracarboxylic-3,4-anhydride-9,10-imide (9).** A solution of 1,6,7,12-tetra(4-*tert*-butylphenoxy)-perylene-3,4,9,10-tetracarboxylic dianhydride[49] (3.0 g, 3.20 mmol) in toluene (100 mL) was purged with dry nitrogen for 15 min and then was heated to reflux. To this solution, *n*-butylamine (0.32 mL, 3.2 mmol) in toluene (10 mL) was slowly added over the course of 30 min. The resulting mixture was refluxed continuously for another 30 min, and then the volatiles were removed under reduced pressure. The residue was purified by column chromatography on silica gel with chloroform as the eluent. Repeated chromatography followed by recrystallization from a mixture of $CHCl_3$ and MeOH gave pure product **9** as a red solid (1.70 g, yield 53.1%); mp > 300 °C; ^{1}H NMR (300 MHz, $CDCl_3$): δ 8.22 (s, 4H), 7.23 (d, J = 7.64 Hz, 8H), 6.82 (d, J = 8.35 Hz, 8H), 4.11 (t, 2H), 1.65 (m, 2H), 1.40 (m, 2H), 1.29 (s, 36H), 0.93 (t, 3H); MALDI-TOF MS(*m*/*z*) 1040.5, calcd for $C_{68}H_{65}NO_9$ (*m*/*z*) 1039.5. Anal. Calcd for $C_{68}H_{65}NO_9$: C, 78.51; H, 6.30; N, 1.35. Found: C, 78.39; H, 6.38; N, 1.36.

Trimer 1. A mixture of **7** (120 mg, 0.15 mmol), **6** (10 mg, 0.025 mmol), and imidazole (3.0 g, 44.05 mmol) in toluene (15 mL) was refluxed under N_2 for 10 h. After the solvent was evaporated, the residue was dissolved in chloroform and washed with water to remove the imidazole. The chloroform was then removed under reduced pressure, and the residue was purified by column chromatography on silica gel using 1000:5 v/v $CHCl_3$/MeOH as the eluent. Trimer **1** is collected as red-purple solid (37 mg, 58%); mp > 300 °C; ^{1}H NMR (300 MHz, $CDCl_3$): δ 9.21 (br, 6H), 8.38 (br,3H), 8.33 (br, 3H), 8.12 (br, 3H), 8.03 (br, 3H), 6.82−7.65 (br, 39H), 4.15 (t, 6H), 1.75 (br, 6H), 1.40 (s, 54H), 1.26−1.39 (br, 6H), 0.90 (br, 9H); MALDI-TOF MS (*m*/*z*) 2577, calcd for $C_{165}H_{138}N_{12}O_{18}$ (*m*/*z*) 2576. Anal. Calcd for $C_{165}H_{138}N_{12}O_{18}$: C, 76.90; H, 5.40; N, 6.52. Found: C, 76.78; H, 5.53; N, 6.36.

Trimer 2. A mixture of **8** (120 mg, 0.196 mmol), **6** (10 mg, 0.025 mmol), and imidazole (3.00 g, 44.05 mmol) in toluene (15 mL) was refluxed under N_2 for 10 h. After the solvent was evaporated, the residue was dissolved in chloroform and washed with water to remove the imidazole. The chloroform was then removed, and the residue was purified by column chromatography on silica gel using 1000:5 v/v $CHCl_3$/MeOH as the eluent. Trimer **2** is collected as a green solid (28 mg, 52%); mp > 300 °C; ^{1}H NMR (300 MHz, $CDCl_3$): δ 9.20 (br, 3H), 9.16 (br,3H), 8.66 (br, 3H), 8.49 (br, 3H), 8.46 (br, 3H), 8.24 (br, 3H), 7.87 (br, 6H), 7.04 (br, 3H), 6.67 (br, 6H), 4.19 (t, 6H), 3.49 (m, 12H), 2.69 (m, 12H), 1.40−1.70 (m, 48H), 1.00−1.50 (t, 9H); MALDI-TOF MS (*m*/*z*) 2186.9, calcd for $C_{135}H_{120}N_{18}O_{12}$ (*m*/*z*) 2185.9. Anal. Calcd for $C_{135}H_{120}N_{18}O_{12}$: C, 74.16; H, 5.53; N, 11.53. Found: C, 74.23; H, 5.61; N, 11.33.

Trimer 3. A mixture of **9** (250 mg, 0.241mmol), **6** (15 mg, 0.038 mmol), and imidazole (3.00 g, 44.05 mmol) in toluene (15 mL) was refluxed under N_2 for 10 h. After the solvent was evaporated, the residue was dissolved in chloroform and washed with water to remove the imidazole. The chloroform was then removed, and the residue was purified by column chromatography on silica gel using 1000:3 v/v $CHCl_3$/MeOH as the eluent. Trimer **3** is collected as a red solid (61 mg, 47%); mp > 300 °C; ^{1}H NMR (300 MHz, $CDCl_3$): δ 8.20 (s, 12H), 7.69 (br, 6H), 7.18−7.08 (br, 33H), 6.81 (br, 24H), 4.13 (t, 6H), 1.38−1.65 (br, 12H), 1.23 (s, 108H), 0.92 (t, 9H); MALDI-TOF MS (*m*/*z*) 3466.5, calcd for $C_{225}H_{210}N_{12}O_{24}$ (*m*/*z*) 3465.5. Anal. Calcd for $C_{225}H_{210}N_{12}O_{24}$: C, 77.97; H, 6.11; N, 4.85. Found: C, 77.83; H, 6.38; N, 4.79.

Acknowledgment. Financial support from the Natural Science Foundation of China (grant nos. 20571049, 20771066, and 20610467), Ministry of Education of China and Shandong University, is gratefully acknowledged.

Supporting Information Available: The synthesis scheme of these PDI trimers. This material is available free of charge via the Internet at http://pubs.acs.org.

LA801463U

(48) Fan, L.; Xu, Y.; Tian, H. *Tetrahedron Lett.* **2005**, *46*, 4443–4447.
(49) Würthner, F.; Sautter, A.; Schilling, J. *J. Org. Chem.* **2002**, *67*, 3037–3044.